Received: 22 March 2021 | Accepted: 19 August 2021

DOI: 10.1111/2041-210X.13715

Methods in Ecology and Evolution BRITISH ECOLOGICAL SOCIETY

RESEARCH ARTICLE

A novel and efficient method for wood–leaf separation from terrestrial laser scanning point clouds at the forest plot level

Peng Wan[1] | **Jie Shao**[2] | **Shuangna Jin**[3] | **Tiejun Wang**[4] | **Shengmei Yang**[1] | **Guangjian Yan**[3] | **Wuming Zhang**[2]

[1]Changjiang River Scientific Research Institute (CRSRI), Wuhan, China

[2]School of Geospatial Engineering and Science, Sun Yat-sen University, Zhuhai, China

[3]Faculty of Geographical Science, Beijing Normal University, Beijing, China

[4]Faculty of Geo-Information Science and Earth Observation (ITC), University of Twente, Enschede, The Netherlands

Correspondence
Jie Shao
Email: shaoj9@mail.sysu.edu.cn

Wuming Zhang
Email: zhangwm25@mail.sysu.edu.cn

Funding information
National Natural Science Foundation of China, Grant/Award Number: 41971380 and 42001374; Guangxi Natural Science Fund for Innovation Research Team, Grant/Award Number: 2019GXNSFGA245001

Handling Editor: Hooman Latifi

Abstract

1. With the increasing use of terrestrial laser scanning (TLS) technology in the field of forest ecology, a large number of studies have been carried out on the separation of wood and leaves based on TLS point cloud data. However, most wood–leaf separation methods adopt the point-wise classification strategy, which is not efficient for processing large-volume TLS datasets acquired at the forest plot level.
2. In this study, we proposed a segment-wise classification strategy to improve the efficiency of the wood–leaf separation from large-volume TLS point cloud datasets collected at the forest plot. The proposed method first decomposes the point cloud into three parts based on the threshold values of its local curvature. Then, the first two parts with lower local curvatures were segmented respectively by a connected component labelling algorithm. Finally, the segmented point clouds were classified into wood or leaf segments according to the segment-wise geometric features of each segment. We tested our method on both needleleaf and broadleaf forest plots in temperate and tropical forests. We also compared our method with two other state-of-the-art wood–leaf separation methods, that is, the CANUPO and LeWoS.
3. The results showed that our method was more than 10 times faster than the compared methods while maintaining comparable and even higher accuracy.
4. Our study demonstrates that the segment-wise classification strategy applies to the large-volume TLS datasets and can greatly improve the efficiency of the classification. The proposed method is simple, fast and universally applicable to the TLS data from various tree species and forest types at the plot level, which may facilitate the adoption of TLS technology by forest ecologists in their studies.

KEYWORDS

computational efficiency, forest ecology, point-wise classification, segment-wise classification, terrestrial LiDAR

1 | INTRODUCTION

Tree architecture, for example, the stem form, branching pattern, and spatial distribution of leaves, directly influences tree photosynthesis and evapotranspiration and ultimately affects carbon and water storage in forests (Lau et al., 2018). It is important to quantify the variation in tree architecture among species to understand how tree architecture relates to the physiological function of trees (Disney et al., 2018).

However, accurate quantification of the tree architecture using manual measurements is challenging and time-consuming (Quammen, 2012).

Terrestrial laser scanning (TLS) is an effective technology for collecting dense and highly detailed three-dimensional (3D) point clouds of trees. Point clouds can be used for the quantitative analysis of tree architecture characteristics, such as branching structures (Pyörälä et al., 2018) and stem curves (Liang et al., 2013). Wood–leaf separation is a prerequisite step to reconstructing the quantitative tree models from TLS data (Raumonen et al., 2013) and estimating the canopy gap fraction and leaf area index (Chen et al., 2018). However, accurate and efficient separation of wood and leaf points from TLS data remains a challenging task. Over the last decade, various types of methods have been proposed to address this issue, which has become a hot topic of research in recent years.

In general, the types of classification features used in wood–leaf separation include radiometric features, waveform features and geometric features. Radiometric features refer to the intensity and reflectivity of laser returns at specific wavelengths. Côté et al. (2009) differentiated wood and leaf points based on the intensity of laser returns. The point intensity threshold values for distinguishing wood and leaves were chosen manually. It is known that the intensity of laser returns is related not only to the spectral properties of the target but also to the incidence angle, the travelling distance of the laser beam (Kukko et al., 2008) and the roughness of the reflecting surface (Pesci & Teza, 2008). Hence, radiometric calibration of point intensity is also a complex issue. In the last few years, some state-of-the-art TLS equipment has been developed. Yao et al. (2011) and Yang et al. (2013) used the relative widths of the returned waveform to separate the wood and leaf points. Danson et al. (2014) tested a dual-wavelength full-waveform TLS, and Li et al. (2013) explored the feasibility of a multi-wavelength laser scanner for wood–leaf separation. However, the use of dual-wavelength and full-waveform information is limited by the availability of the equipment.

The most recently developed methods are dependent on geometric features. Geometric features are the size, shape, location, density, roughness, curvature and other characteristics of a point set, which calculated from the 3D coordinates of the points. Unlike radiometric features, the geometric feature uses information about the position of the laser points. Some methods dependent on geometric features have been proposed for individual trees and others have been developed for forest plots. For individual trees, Tao et al. (2015) developed a method based on the circular detection in point slices and the algorithm of the shortest path. Tao's method applies only to individual trees due to the limitation of the shortest-path algorithm. Similarly, the shortest-path algorithm has also been used for wood–leaf separation in the methods proposed by Xu et al. (2007), Livny et al. (2010) and Vicari et al. (2019). Raumonen et al. (2013) proposed a wood–leaf separation method that the point cloud was first segmented into small non-overlapping cover sets, and then the cover sets were classified based on their geometric features. Wang et al. (2017) compared four machine learning classifiers for the wood–leaf separation of individual trees based on both geometric and radiometric features. The results showed that the machine learning classifiers can achieve high accuracy for wood–leaf separation on individual trees. Furthermore, Wang et al. (2020) proposed an unsupervised classification method (i.e. LeWoS) for the wood–leaf separation using a graph-based segmentation technique with point cloud density and point-wise geometric features. They tested the LeWoS on 61 individual large tropical trees and reached an average value of 91.59% of classification accuracy.

For forest plots, methods based on machine learning algorithms are more frequently used. Lalonde et al. (2006) introduced a point cloud classification method by fitting a Gaussian mixture model to manually labelled training data. Ma et al. (2016) improved Lalonde's method by adding two additional filters based on geometric information. Brodu and Lague (2012) proposed the CANUPO method, which extends local geometric features to multiple scales. Zhu et al. (2018) combined various local geometric features and radiometric features to separate foliar and woody materials by using a random forest classifier. In addition, the deep learning method was also introduced for wood–leaf separation (Xi et al., 2018). Table 1 shows a summary of the abovementioned methods.

Although some methods based on geometric features and machine learning have achieved good accuracy on wood–leaf separation, the main drawbacks of this type of methods are their high computational demands for processing TLS datasets at the forest plot level (Liang et al., 2012). Here, we aim to propose a segment-wise classification method for the accurate and efficient separation of wood and leaves from TLS data at the plot level. We test our method on both needleleaf and broadleaf forest plots in temperate and tropical forests. We also compare our method with two other state-of-the-art methods, that is, the CANUPO and LeWoS.

2 | MATERIALS AND METHODS

2.1 | Forest plots

We tested the proposed method on the TLS datasets collected from three forest plots of different stem density, topography and tree species, that is, a white birch *Betula papyrifera* plot, a Dahurian larch (DL) *Larix gmelinii* plot and a Chinese scholar tree (CST) *Styphnolobium japonicum* plot. The white birch plot (WB) includes 21 white birches on a slope of approximately 22 degrees, the size of the WB plot is 15 m × 30 m. The DL plot includes 15 trees on flat terrain, the size of the DL plot is 15 m × 15 m. The CST plot includes 37 trees on flat terrain, the size of the CST plot is 30 m × 30 m. Figure 1 shows the actual condition of each sample forest plot when the TLS datasets were collected. The mean diameter at breast height and tree height, stem density and the density of understory vegetation of each sample plot are summarized in Table 2.

2.2 | TLS datasets

The TLS datasets were collected in July 2018 by using a Riegl VZ-1000 (Riegl GmbH) terrestrial laser scanner. The scan angle

TABLE 1 List of published methods for wood–leaf separation from terrestrial laser scanning data

Authors (published year)	Applicable scenarios	Method categories	Reported mean accuracies
Wang et al. (2020)	Individual trees or forest plots	# Point-wise segmentation # Geometric features # Segment-wise classification	91%
Vicari et al. (2019)	Individual trees	# Shortest-path analysis # Geometric features # Point-wise classification	Simulated data: 83% Field data: 89%
Xi et al. (2018)	Forest plots	# Deep 3D FCN* # Point-wise classification	94%
Ferrara et al. (2018)	Individual trees	# Unsupervised # Geometric feature # Point-wise classification	96% (Cork oak) trees
Zhu et al. (2018)	Forest plots	# Random forest # Radiometric and Geometric features # Point-wise classification	84.40% 4 beech broadleaf 2 spruce coniferous Four mixed
Wang et al. (2017)	Individual trees	# Machine learning methods # Radiometric and geometric features # Point-wise classification	Support vector machine: 93.5% Naïve Bayes: 89% Random forest: 96% Gauss mixture model: 91%
Ma et al. (2016)	Forest plots	# Gauss mixture model and six additional filters # Geometric features # Point-wise classification	94% Douglas fir
Tao et al. (2015)	Individual trees	# Shortest-path analysis # Geometric features # Point-wise classification	84% Camphor tree Magnolia tree
Li et al. (2013); Danson et al. (2014)	Forest plots	# Multi-wavelength intensity # Point-wise classification	No reports
Côté et al. (2009); Wu et al. (2013)	Individual trees	# Intensity # Point-wise classification	No reports
Yao et al. (2011); Zhao et al. (2011); Yang et al. (2013)	Forest plots	# Return waveforms # Point-wise classification	No reports
Brodu and Lague (2012)	River bed	# Support vector machine # Multi-scales geometric features # Point-wise classification	98%
Raumonen et al. (2013)	Individual trees	# Unsupervised # Geometric features # Segment-wise classification	No reports
Xu et al. (2007); Livny et al. (2010)	Individual trees	# Shortest-path analysis # Geometric features # Point-wise classification	No reports
Lalonde et al. (2006)	Forest plots	# Gauss mixture model # Geometric features # Point-wise classification	83%~93%

Note: FCN refers to the **F**ully **C**onvolutional **N**etwork.

resolution was 0.03 degrees, and the vertical and horizontal scanning ranges were 30–130 degrees and 0–360 degrees, respectively. In each sample forest plot, five to seven scans were implemented at the centre and the periphery of the plots. All scans were registered together using the RiSCAN Pro software package (Riegl GmbH). The registered point clouds were clipped manually to exclude trees outside each plot (Figure 2).

The proposed method was also tested on an open-access TLS dataset, which downloaded from the Dryad Digital Repository https://doi.org/10.5061/dryad.np5hqbzp6 (Di Wang et al., 2020). The open-access TLS dataset was collected from a tropical forest in Eastern Cameroon, which includes 106 tropical trees within a 110 m × 90 m plot and over 180 million points. The wood and leaf points were manually labelled, and the ground points and

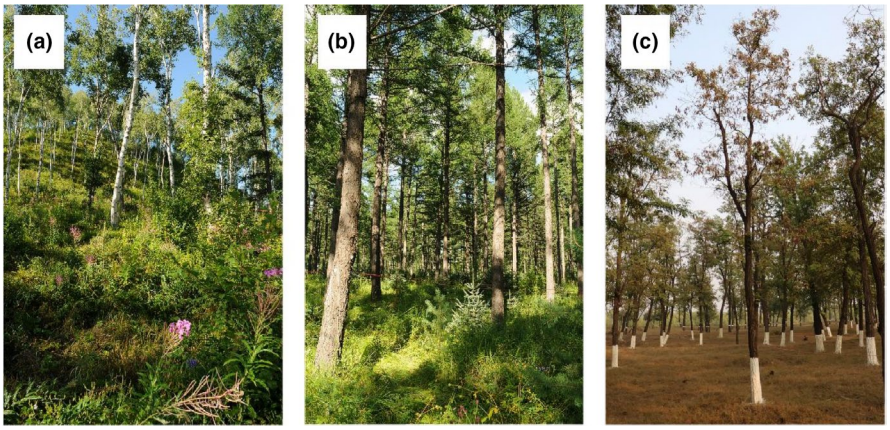

FIGURE 1 The forest condition of each sample forest plot. (a) The white birch plot. (b) The Dahurian larch plot. (c) The Chinese scholar tree plot

Forest plot	Stem density (stems/ha)	Mean diameter at breast height (cm)	Mean tree height (m)	Understory vegetation
White birch	467	19.34	13.38	Dense
Dahurian larch	667	28.33	14.23	Moderate
Chinese scholar tree	411	24.2	10.66	Sparse

TABLE 2 The characteristic of the sample forest plots

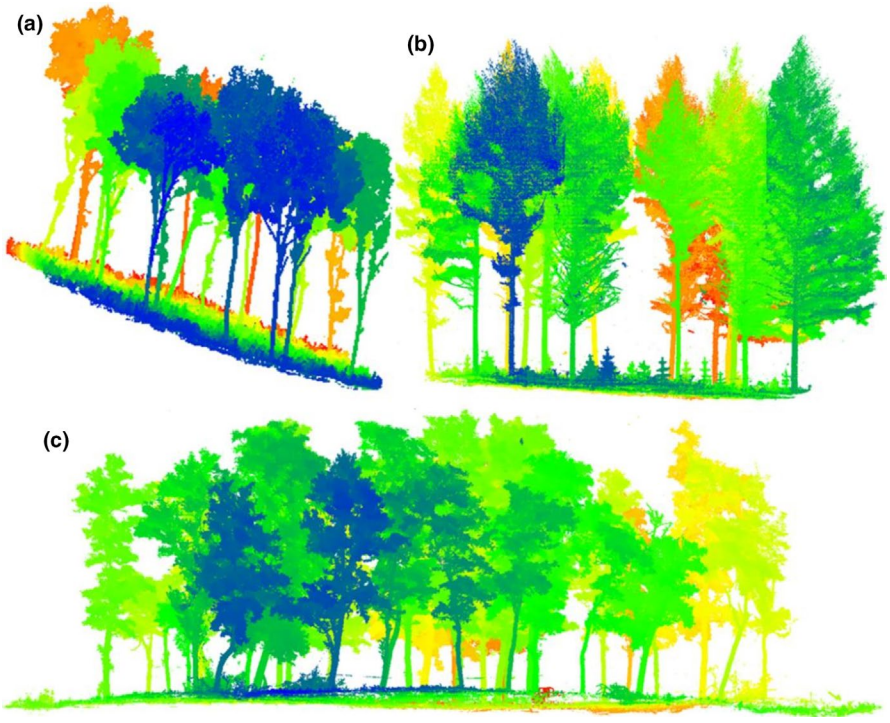

FIGURE 2 Three field-collected terrestrial laser scanning datasets. (a) White birch plot. (b) Dahurian larch plot. (c) Chinese scholar tree plot

understory vegetation points were already removed by the data provider (Figure 3).

2.3 | Wood–leaf separation

2.3.1 | Overview of the proposed method

The proposed method adopted a segment-wise classification strategy. The point clouds were segmented by using a connected component segmentation algorithm, then were classified into wood or leaf segment-by-segment based on their geometric features. However, for the raw point clouds, it is not possible to obtain an effective segmentation result only by a connected component segmentation algorithm because of the very high density of the TLS point clouds and the tight connections between wood and leaf points. An effective segmentation for the classification purpose is that the point cloud was segmented into pure segments, which consist of a single classification target, that is, the wood and leaf point. Therefore, we introduced a point cloud decomposing step before

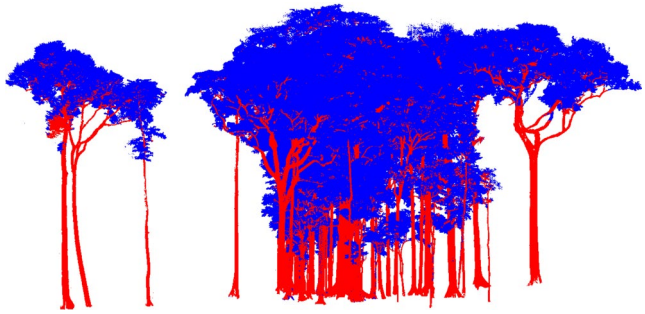

FIGURE 3 The manually labelled open-access terrestrial laser scanning dataset. The red points refer to wood points and the blue points refer to leaf points

segmentation to divide the point cloud into two or three parts to reduce the point density and break the connections between wood and leaf points. Figure 4 shows the overall workflow of the proposed method.

The following subsections detailed methods used in the main steps shown in the flowchart.

2.3.2 | Ground filtering

Ground filtering was a prerequisite step in the proposed method for reducing the data volume and breaking the ground connection between stems. In this study, we adopted an open-source ground filtering algorithm (Zhang et al., 2016), cloth simulation filtering, for its fast processing speed and reliable results.

2.3.3 | Point cloud decomposing

The method of point cloud decomposing was based on the local curvature calculated from a point and the points around it within a certain neighbourhood. After traversing all the points, each point was assigned a local curvature value, which essentially represents the curvature characteristics of a point set within a sphere centred on a point. Local curvature can be used to roughly separate tree components (Zhang et al., 2019). The points on stems and boughs usually have the smallest local curvatures due to their large diameters and regular point distribution. The branches and twigs, which have smaller diameters and are surrounded by leaves, usually have moderate local curvatures. The leaf points usually have the largest local curvatures because of their scattered distribution pattern and canopy gaps. In this study, the surface variation (SV) was adopted as a curvature feature to divide the point cloud into three parts. The SV was proposed by Pauly et al. (2002) to quantitatively describe the variation along the surface normal, that is, estimates how much the points deviate from the tangent plane. It should be noted that the SV is not an estimation of surface curvature based on function fitting, but a simplification index of the surface curvature. The SV is defined by Equation (1). For a point $p_n = (x_n, y_n, z_n)$ and the points around it within a neighbourhood $p_i = (x_i, y_i, z_i)_{i=1}^{n}$, the calculation of the SV was based on the eigenvalues of principal component analysis, which was defined as

$$\mathrm{SV}(p_n) = \frac{\lambda_2}{\lambda_0 + \lambda_1 + \lambda_2}, \quad (1)$$

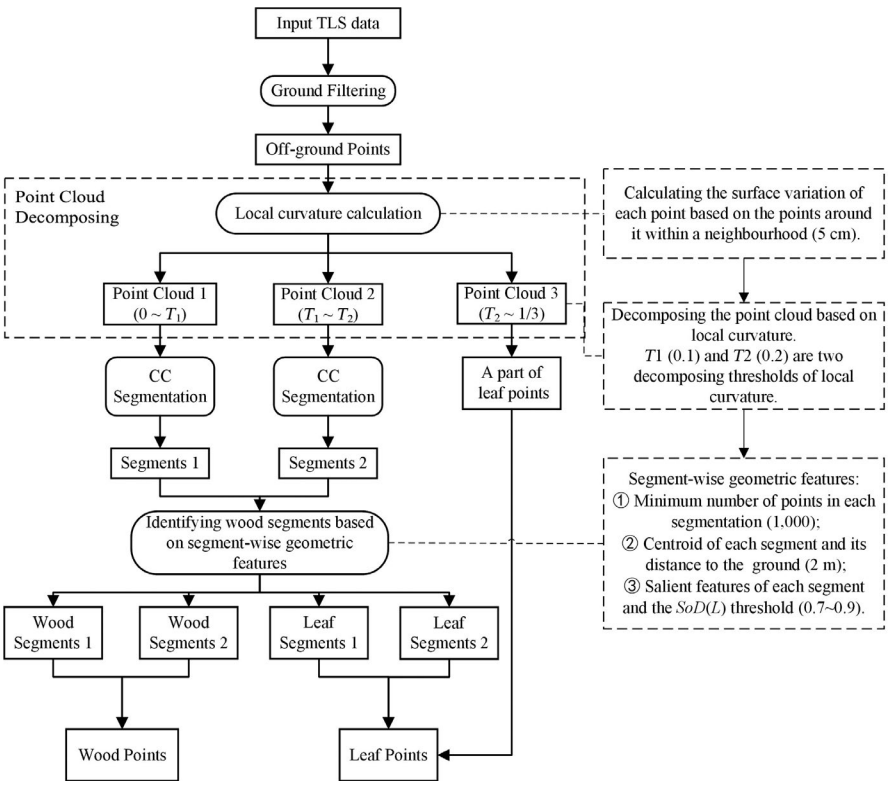

FIGURE 4 The overall workflow of the proposed method. The left column shows the steps of the method, and the right column shows the annotation of each main step. The numbers in the bracket are the parameters set in this study. The SoD(*L*) refers to the significance of the difference of linear salient feature (Equation 4)

where λ_k ($k = 0, 1, 2$) are the eigenvalues of a covariance matrix C sorted in descending order as $\lambda_0 \geq \lambda_1 \geq \lambda_2$. The covariance matrix C is defined as

$$C_{3\times3} = \frac{1}{n}\sum_{i=1}^{n}(p_i - \overset{!!}{p})(p_i - \overset{!!}{p})^{\mathrm{T}}, \quad (2)$$

where $\overset{!!}{p} = (1/n)\sum_{i=1}^{n}(p_{xi}, p_{yi}, p_{zi})$ is the geometric centre of P. n is the number of points within a neighbourhood of an arbitrary reference point. The neighbourhood size was set as 5 cm in this study.

The SV has a limited range from 0 to 1/3 for any point. To divide the point cloud into three parts, two thresholds (T_1, T_2) of the SV were chosen according to experiments in previous studies (Zhang et al., 2019), that is, T_1 was set to 0.1, and T_2 was set to 0.2. The same set of thresholds was adopted for all sample plots. For example, Figure 5 shows the three parts of the divided point cloud of an individual tree. The first part, in which the SV of points ranged from 0 to 0.1, comprised almost all the stem points, most of the branch points and nearly half of the leaf points. The second part, in which the SV ranged from 0.1 to 0.2, was mainly composed of leaf points and a fraction of branch points. The third part, in which the SV ranged from 0.2 to 1/3, was composed of leaf points. The first and second parts that contained wood points were used in the next step for segmentation.

2.3.4 | Segmentation of connected components

After decomposing the point cloud into three parts, the first two parts, which have smaller local curvature were segmented separately. We used a connected component segmentation algorithm to segment the point cloud into segments. Connected component segmentation is a simple and fast algorithm based on the proximity of points. As shown in Figure 6, the point clouds were first voxelized using 3D grids by building an octree. Then, the 3D grids that contained at least one point were assigned a value of 1. The vacant 3D grids were assigned a value of 0. Finally, the points in adjacent grids with a value of 1 were merged into the same segment. The vacant grids with a value of 0 became the gaps between the segments. The size of the 3D grids determined how many segments were produced and how small the segments were. Smaller grids make it easier to identify the gaps between leaves and branches and separate them. However, reducing the grid size by every two times leads to an increase in the number of segments by approximately eight times and will significantly increasing the calculation time. We set the grid size to a compromise value (0.01 m) in this study, which is just small enough to separate the leaves from the branches. The optimum grid size is related to the density of the point cloud and the tree species, it is difficult to find a suitable grid size based on the average spacing between leaves and branches just by theoretical analysis. The grid size used in this study is the optimum value obtained through several tests.

In addition, the minimum number of points within per segment (Min. NoP) is a parameter that should be set in the connected component segmentation. We set the Min. NoP as 1,000 in this study. The segments containing <1,000 points will be classified as leaf segments directly. Similar to the grid size, Min. NoP is also an empirical threshold derived from several tests. Increasing the value of Min. NoP will cause more branches to be classified into leaves, and conversely, more leaves will be classified into branches.

2.3.5 | Geometric features

We introduced two geometric features to identify the wood segments, that is, the salient features and the distance between the geometric centre of each segment and the ground. The salient features were the main features used for the wood–leaf separation, and the distance feature was used to remove the understory vegetation.

Salient features

The salient features are a set of geometric features based on principal component analysis. Similar to the calculation of SV, it also requires that the eigenvalues of a covariance matrix of a point set (λ_0, λ_1, λ_2) are first obtained. The salient features quantitatively describe the dominant distribution pattern of a point set as linear, planar and scattered. The scattered points will be indicated as $\lambda_0 \approx \lambda_1 \approx \lambda_2$; The linearly distributed points will be indicated as $\lambda_0 \gg \lambda_1 \approx \lambda_2$; The points distributed on a plane will be indicated as $\lambda_0 \approx \lambda_1 \gg \lambda_2$ (Figure 7).

The salient features have been used in most wood–leaf separation algorithms for TLS data. However, their calculation in existing algorithms is point-wise and based on neighbouring points. This has caused problems with a large amount of computation and inconsistency in the salient features of a point when using different neighbourhood sizes. In our method, we calculated the salient features of each segment rather than each point to significantly reduce the computation amount and avoided the setting of neighbourhood size. The salient features of the points within a segment will be consistent and stable. For the points $p_i = (x_i, y_i, z_i)_{i=1}^{m}$ in each segment, we first calculated their covariance matrix C by using Formula 2. Then, the eigenvalues λ_k ($k = 0, 1, 2$) of C were obtained by singular value decomposition and sorted in descending order as $\lambda_0 \geq \lambda_1 \geq \lambda_2$. Based on the eigenvalues, the salient features of a segment can be defined as (Demantke et al., 2011)

$$L = \frac{\sqrt{\lambda_0} - \sqrt{\lambda_1}}{\sqrt{\lambda_0}}; P = \frac{\sqrt{\lambda_1} - \sqrt{\lambda_2}}{\sqrt{\lambda_0}}; S = \frac{\sqrt{\lambda_2}}{\sqrt{\lambda_0}}, \quad (3)$$

where L, P and S refer to the linear feature, planar feature and scattered feature, respectively, and $L + P + S = 1$. λ_0, λ_1, λ_2 are the covariance matrix of a segment.

Figure 8 shows an example of connected component segmentation and the salient features of the segments. It can be found that the stem segment and branch segment were all dominated by the linear feature, which has significantly higher values than the other

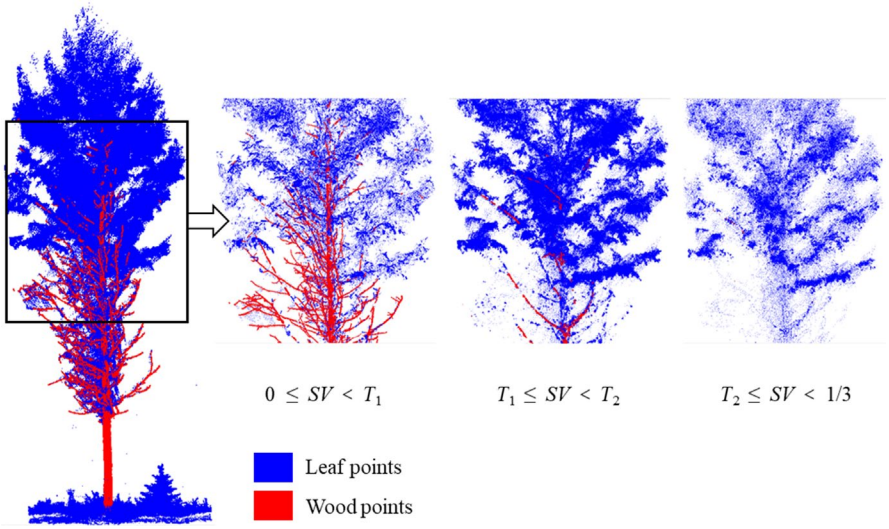

FIGURE 5 An example of the decomposed point cloud. T_1 and T_2 refer to the thresholds of the surface variation (SV). In this example, T_1 equals 0.1, T_2 equals 0.2. The wood and leaf points were labelled manually

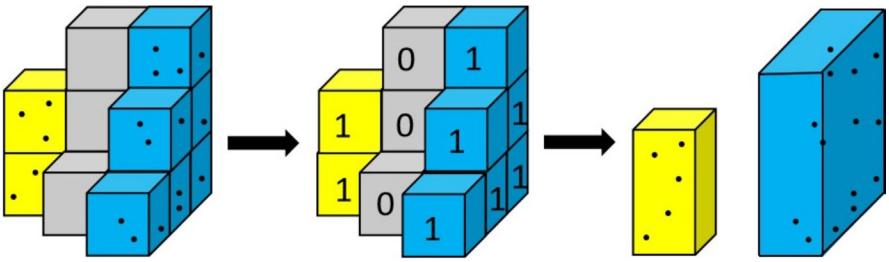

FIGURE 6 Schematic diagram of the connected component segmentation. Here, a point cloud was segmented into two segments

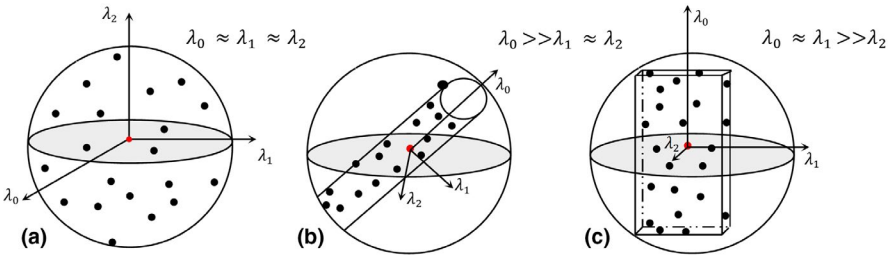

FIGURE 7 Diagram to illustrate the salient features of three different spatial distribution patterns. λ_0, λ_1, λ_2 are the covariance matrix of a point set. (a), (b) and (c) illustrate the spatial distribution pattern of a point set as scattered, linear and planar, respectively

two features. In contrast, the leaf segment has no dominant feature. Therefore, the segments dominated by the linear feature can be labelled as wood segments. In this study, we introduced an index, that is, the **S**ignificance **o**f **D**ifference (SoD), to evaluate the significance of the linear/planar/scattered features among the three salient features. In general, the most straightforward way to evaluate the significance of a feature is by using the value of that salient feature. However, even if that feature has the same value, there may be differences in the level of significance between features. For example, when we look for linear features, the following two cases may arise: (a) $L = 0.50$, $P = 0.45$, $S = 0.05$; (b) $L = 0.50$, $P = 0.25$, $S = 0.25$. Although the value of the linear salient feature (L) is the same in both cases, it is clear that the latter linear feature is more significant because it is easier to distinguish. So, to address the issue of assessing relative significance levels, we constructed the index SoD. Specifically, the SoD of the linear feature was defined as

$$\mathrm{SoD}(L) = L + (1 - L) \times [L - max(P, S)], \quad (4)$$

where L, P and S refer to the **L**inear feature, **P**lanar feature and **S**cattered feature, respectively.

The SoD(L) is an index ranging from −1 to 1. When its value is <0, it means that one of the other two salient features is more significant, and when its value is greater than 0, it means that the linear salient feature is more significant. The larger the value of the SoD(L), the more likely it is that a segment is dominated by a linear feature. The user can set its value more intuitively by analogizing it to a confidence level or probability. In this study, segments with the SoD(L) > 0.7 were considered as wood segments. The setting of 0.7 was a conservative threshold for retaining the wood segments as much as possible.

The distance between the geometric centre of each segment and the ground

Understory vegetation, such as grass and small shrubs, is hard to remove from a point cloud based on geometric features. This is because some ground vegetation also has stems that may be wrongly recognized as tree branches.

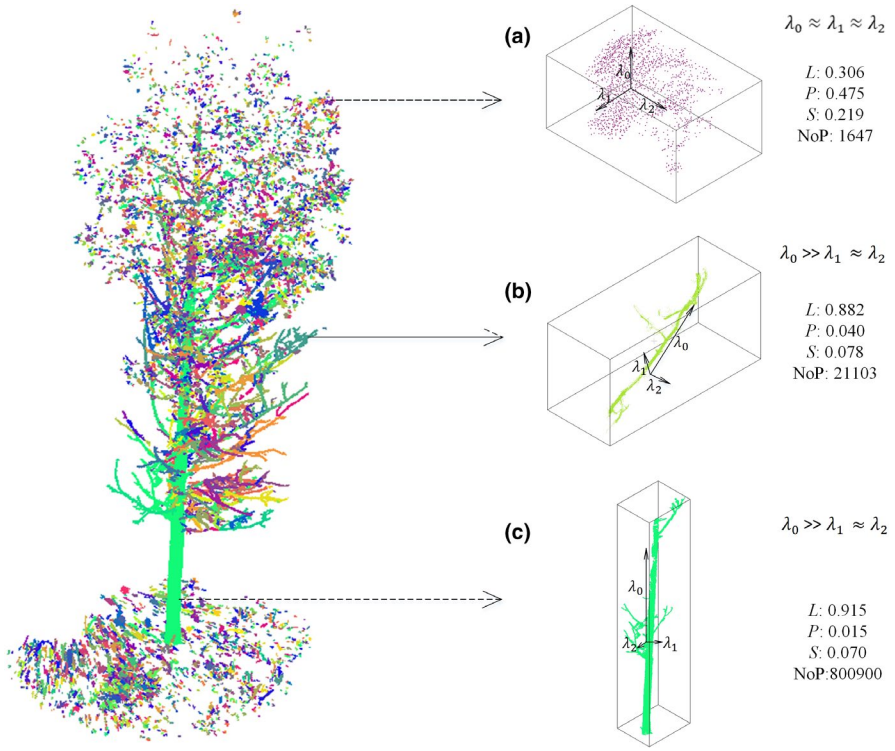

FIGURE 8 An example of the connected component segmentation and the salient features of the segments. The different colours were drawn for the different segments. *L*, *P*, *S* and NoP refer to the attribute value of the linear feature, planar feature, scattered feature and the number of points of each segment. λ_k ($k = 0, 1, 2$) are the eigenvalues of each segment. (a), (b), and (c) illustrate the connected component segmentation results of the leaf, branch, and stem, respectively

TABLE 3 The calculation of accuracy evaluation indexes

	Result			
Reference	**Wood**	**Leaf**		**Error (%)**
Wood	a	b	$f = (a + b)/n$	Type I error: $b/(a + b)$
Leaf	c	d	$g = (c + d)/n$	Type II error: $c/(c + d)$
	$h = (a + c)/n$	$a\_i = (b + d)/n$		
	$n = (a + b + c + d)$			Total error: $(b + c)/n$
	pra $= (a + d)/n$; pre $= f \times h + g \times a\_i$			Kappa: (pra − pre)/(1 − pre)

Note: The *a*, *b*, *c* and *d* refer to the number of points.

Although ground vegetation can be entirely removed by setting a threshold of distance to the DTM, the true stem points on tree stumps may also be wrongly removed in this procedure. For point-wise wood–leaf separation algorithms, it is difficult to solve this problem. However, for the segment-wise classification method, we can easily recognize segments as ground vegetation based on the geometric centre of the segments. The geometric centre of the segments of trees would possess larger distances from the ground surface. For example, points near the ground surface would be classified as wood points if they belong to a segment that has a higher geometric centre. The distance to the ground surface is an input threshold of the proposed method and was set to 1 m in this study. The geometric centre of the segments can be calculated by using the formulas shown in Section 2.3.3.

2.3.6 | Merging the wood segments

Following the procedures shown in Figure 2, we identified the wood segments by their geometric features. The input parameters have been introduced in the sections above. As mentioned in Section 2.3.3, the point cloud was decomposed into three parts, and the third part was composed of leaf points. We used the proposed wood–leaf separation algorithm separately to the first and second parts of the point cloud. After connected component segmentation, the segments identified in the first and second parts were in separate segment groups, that is, segments 1 and segments 2. Then, we merged the extracted wood segments from the two groups of segments.

2.4 | Performance evaluation

2.4.1 | Classification accuracy and processing time

The accuracy of the wood–leaf separation method was evaluated by the percentage of error-classifying points against the referenced classification results. The references were acquired by visual inspection. Three types of error (type I error, type II error

TABLE 4 Comparison of accuracy between the CANUPO and the proposed method

Datasets	Methods	Type I error (%)	Type II error (%)	Total error (%)	Kappa (%)
White birch	CANUPO	14.77	8.08	8.89	64.93
	Our method	10.02	4.75	5.39	77.11
Dahurian larch	CANUPO	16.07	7.54	9.32	73.02
	Our method	8.85	3.66	4.74	85.90
Chinese scholar tree	CANUPO	18.41	8.99	10.50	65.02
	Our method	21.46	2.98	5.93	77.38

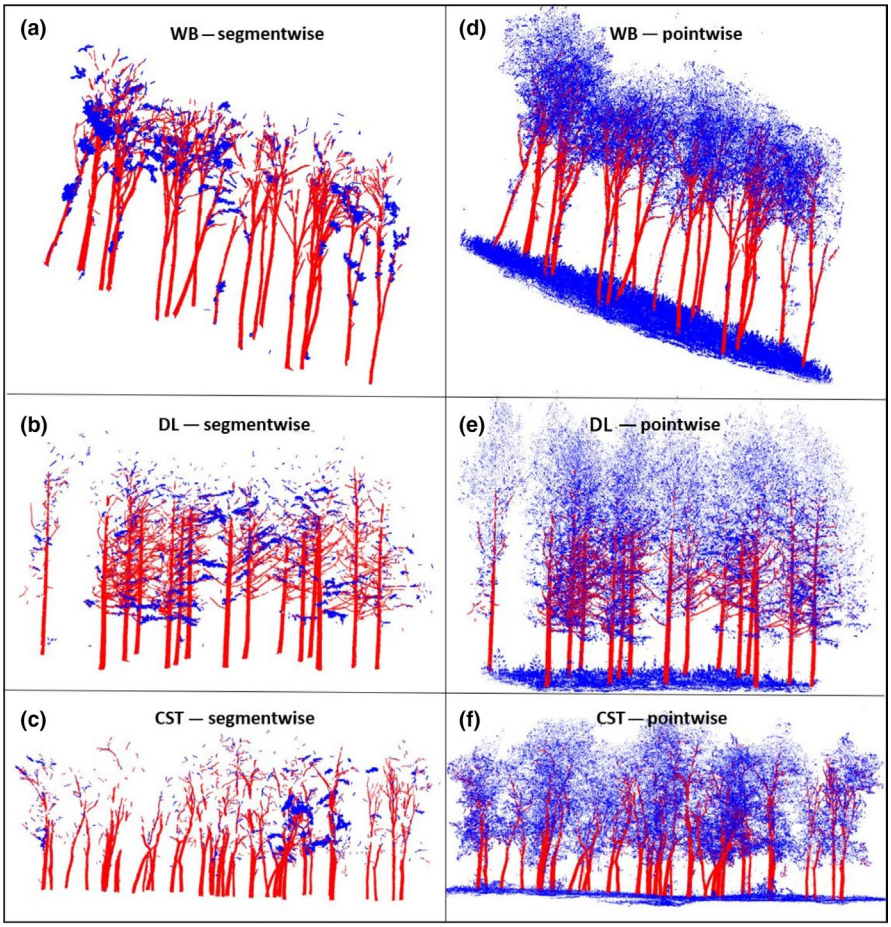

FIGURE 9 Visualization of the extracted wood points of the CANUPO (point-wise) and our method (segment-wise). WB, DL and CST represent the datasets of white birch, Dahurian larch and the Chinese scholar tree, respectively. The red points refer to the wood points, which correctly classified, the blue points refer to the leaf points, which incorrectly classified into wood points. (a), (b) and (c) shows the classification results of the datasets of WD, DL and CST, respectively, from our method. (d), (e) and (f) shows the classification results of the datasets of WD, DL and CST, respectively, from the CANUPO method

and total error) and the kappa coefficient were quantified. The type I error, also known as the omission error, was defined as the number of wood points that were wrongly classified as leaf points divided by the number of referenced wood points. The type II error, also known as commission error, was the number of leaf points that were wrongly classified as wood points divided by the number of referenced leaf points. The total error was the number of wrongly classified points divided by the total number of points. The Kappa coefficient was calculated from the statistics of the wrongly classified points. The calculation of accuracy indexes is shown in Table 3.

In addition, the processing times were recorded to assess the time efficiency of the wood–leaf separation algorithms. All tests were conducted on a typical desktop computer with an Intel Core i7-6700 CPU (3.40 GHz) and 16 GB of RAM.

2.4.2 | Method comparison

To compare the difference in performance between the proposed method and the point-wise classification methods, we processed all the field-collected sample datasets using a point-based method proposed by Brodu and Lague (2012), CANUPO. The reason for adopting Brodu's method for the comparison is that (a) it is a point-based method using only geometric features that have reported good classification accuracy (98%) in the literature; (b) it adopts multi-scale geometric features to improve the results, which were more robust than the algorithms using single-scale and double-scale geometric features; (c) it is based on machine learning classification algorithms and thus is representative of many supervised classification methods and (d) it has free and open-source codes which are easy to access. Therefore, the CANUPO was very

suitable for the performance evaluation of the proposed method in this study.

We also compared the proposed method to the LeWoS, a wood–leaf separation method proposed by Wang et al. (2020) on the open-access TLS dataset. The LeWoS first adopt a graph-based point cloud segmentation technique and exercise it iteratively and classify the segmented point cloud using a class probability estimation. Finally, they apply graph-structured class regularization that operates on the class probability to achieve a spatially smooth classification result. The reason for adopting the LeWoS for comparison is that (a) it is a newly proposed state-of-method and (b) the LeWoS used a segmentation-based classification strategy, which is similar to the basic idea of our proposed method.

3 | RESULTS

3.1 | Classification accuracy

Table 4 shows the comparison of the accuracy of the CANUPO and our method on the three field sample plots. The results show that the classification accuracy of the proposed method was higher than that of the point-wise method in all sample plots. The total errors of the proposed method in the three sample plots were 5.39%, 4.74% and 5.93%, respectively, while they were 8.89%, 9.32% and 10.05% in the CANUPO, respectively. On average, the errors of the CANUPO were 1.76 times greater than those for the proposed method. The Kappa coefficients showed a similar trend, that is, the classification accuracy derived from our method was consistently higher than that obtained from the CANUPO method.

Figure 9 shows the results of the CANUPO and our method on the three field-collected sample plots. It is easy to see that fewer leaf points were wrongly classified as wood points using the proposed method compared with the CANUPO. There were some differences between the two methods in the spatial distribution of the classification errors. The residual leaf points were distributed mainly around the branches in the results of the proposed method; however, the residual leaf points were uniformly distributed in CANUPO's results.

It should be noted that the ground points have been removed during the ground filtering step, thus the blue points under canopies showed in Figure 8 stand for the points on understory vegetation, such as glass and shrub. The CANUPO method cannot separate the understory vegetation points from leaf points. In contrast, the proposed method can filter out the understory vegetation points according to the distance between the geometric centre of the segment and the ground, so there were seldom residual understory vegetation points in the wood points.

For the open-access TLS dataset provided by Wang et al. (2020), our method achieved a classification accuracy with 16.69% type I error, 3.89% type II error, 7.76% total error and 81.19% kappa coefficient, which means that 92.24% points were being correctly classified (Figure 10). In contrast, the LeWoS achieved a classification accuracy of 91.59% on the same TLS data (Di Wang et al., 2020).

FIGURE 10 Visualization of the extracted wood points of our method processed on the open-access terrestrial laser scanning dataset. The red points refer to the wood points which correctly classified, the blue points refer to the leaf points, which incorrectly classified into wood points

3.2 | Time efficiency

In this study, all methods were run on the same desktop computer. The processing time of the CANUPO and LeWoS and our method is shown in Table 6. The processing time does not include the time spent on data reading and writing or parameter tuning, or time spent on sample selection and training in the point-wise method. Table 5 shows a substantial difference in processing time between the methods. Our method required only 2.57 to 18.85 min, whereas the CANUPO required 28.67 to 235.67 min, and the LeWoS was reported 1.5 min for 1 million points, which equivalent to 281.36 min for the entire points of the open-access TLS dataset. The proposed method had a time efficiency of more than 10 times faster than the CANUPO and LeWoS.

4 | DISCUSSION

4.1 | Classification accuracy

In terms of overall classification accuracy, the proposed method achieved better results compared with the CANUPO and LeWoS for all tested datasets in this research, the average classification accuracy of the proposed method reached 94.05%. In reviewing the existing literature, the classification accuracy of wood–leaf separation ranged from 83% to 96% (Table 1), which indicated that the proposed method can provide comparable classification results to the state-of-the-art methods and the segment-wise classification strategy works well with the large-volume TLS data. On the individual tree level, the best classification accuracy was up to 96% (Ferrara et al., 2018; Wang et al., 2017). On the forest plot level, this study reported the highest average classification accuracy to date.

It can be inferred from the results of this study that general-purpose algorithms for point cloud classification face challenges when performing plot level wood–leaf separation. The CANUPO can separate rocks and vegetation with 98% classification accuracy in the riverbed scenes (Brodu & Lague, 2012), however, when faced

TABLE 6 Comparison of the time spent between wood–leaf separation methods

Datasets	Total number of points	Methods	Time cost (min)
White birch	44,205,362	CANUPO	146.22
		Our method	3.5
Dahurian larch	65,209,008	CANUPO	235.67
		Our method	14.41
Chinese scholar tree	25,311,712	CANUPO	28.67
		Our method	2.57
Open-access terrestrial laser scanning dataset	187,571,510	LeWoS	281.36
		Our method	18.85

TABLE 5 Comparison of accuracy between the LeWoS and the proposed method

Datasets	Methods	Type I error (%)	Type II error (%)	Total error (%)	Kappa (%)
Open-access terrestrial laser scanning dataset	LeWoS	10.51	7.51	8.41	80.43
	Our method	16.69	3.89	7.76	81.19

with wood–leaf separation of forest plots, its classification error reached 10% to 20% (Table 4). The difficulty in separating wood components and leaves lies in two main points. First, thin branches, twigs and leaves in the canopy are mixed that even the human eye has difficulty in distinguishing them. Second, as TLS can only scan trees from the outside of the canopy, branches can be heavily obscured by foliage or by each other, resulting in discontinuous and missing branches in the point cloud. Therefore, this study proposed a method that specifically designed to solve the wood–leaf separation problem of point clouds. Although it is not as applicable to multiple classification problems as the general-purpose algorithm, the segment-wise classification strategy can be adopted by other classification problems, such as tree trunk extraction (Zhang et al., 2019).

An issue that is easily neglected in the study of wood–leaf separation algorithms is the extraction or filtering of understory vegetation. The inevitable presence of understory vegetation in the point clouds acquired in the forest can result in many understory vegetation points remaining in the extracted wood points, which are difficult to filter out. The point-wise classification methods have difficulty in dealing with this problem because they cannot distinguish between trees and understory vegetation (Figure 8). However, the proposed method was able to remove the points of understory vegetation thoroughly. This is because the segment-wise approach allows the height of the centre of the segments to be used as a classification feature.

For a wood–leaf separation method, it is a challenge to balance omission and commission errors. Therefore, when simply evaluating the accuracy of the method, we were concerned with the total error and the Kappa coefficient. However, if specific applications are targeted, we are more concerned with the level of omission and commission errors. For example, when we need wood component volumes, a large number of commission errors can lead to a significant overestimation of wood component volumes (Raumonen et al., 2013), whereas the effect of omission errors is relatively small because the volume of twigs is not large (Dassot et al., 2012). In contrast, when we need the fine structure of tree branches, we need to select the results with a small omission error (Lau et al., 2018). In our experimental results (Tables 4 and 5), two scenarios had relatively small omission errors (type I error, the wood points were wrongly classified as leaf points) and the other two had relatively large omission errors. In terms of the commission errors (type II error, the leaf points were wrongly classified as wood points), the proposed method achieves good results in all four scenarios.

4.2 | Time efficiency

The innovation of this study is to propose a segment-wise classification strategy for the wood–leaf separation of a point cloud, under the premise of ensuring the classification accuracy, the classification speed was significantly improved. Generally, comparing the time efficiency of the wood–leaf separation methods is difficult and therefore few studies have reported on the time spent by the algorithm. Some studies have only given rough processing times, with no detailed data (Brodu & Lague, 2012; Wang et al., 2020). This is mainly because the time efficiency of an algorithm is influenced by the method of programming and the platform on which it runs. This makes the various methods comparable only if the programming methods and running platforms are consistent. In this study, both our method and the CANUPO were implemented based on CloudCompare (Girardeau-Montaut, 2018), and the results were obtained on the same computer. The LeWoS is an algorithm developed using MATLAB, and we used the test results given by the authors of the LeWoS for comparison. Based on the results of the test (Table 6),

our method has improved the time efficiency more than 10 times compared with other methods. This was a significant difference that can only be explained by the method itself. In our method, after the point cloud has been segmented, the number of objects to be classified was greatly reduced, as it changes from points to segments.

In the field of forest ecology research, there is an increasing emphasis on obtaining the 3D structure of each tree in large forest areas (Calders et al., 2020; Xi et al., 2020), which will result in a huge volume of ground-based laser scanning data (Wilkes et al., 2017). This study provides an idea for the wood–leaf separation of large-volume point clouds.

From an ecologist's point of view, the time efficiency may be more important than the accuracy of classification in practice, as the perfect method for 100% correct classification does not yet exist, further manual classification is still necessary. Improving the efficiency of the automatic classification stage is useful for ecologists' work.

4.3 | Further requirements

One of the difficulties faced by the research of the wood–leaf separation algorithm is the acquisition of reference data. It is difficult and time-consuming to separate branches and leaves manually, and it is difficult to guarantee classification accuracy. Some studies have used sampling methods to evaluate classification accuracy (Zhu et al., 2018). This method requires a high level of representation in sample selection, which is often difficult to meet and causes statistical bias. Therefore, opening the reference data of manual classification to the community can promote the research of branch and leaf separation algorithm. We shared our field-collected and manually classified TLS datasets to the public on the Dryad Digital Repository (https://doi.org/10.5061/dryad.rfj6q5799, Wan et al., 2021).

Another way to obtain accurate reference data is to simulate the TLS data on a virtual forest plot. The 3D tree models and virtual forest plot can be built with modelling software for vegetation, such as OnxyTree (http://onyxtree.com/). TLS data simulation can be achieved with data simulation software, such as DART (Gastellu-Etchegorry et al., 2016), LESS (Qi et al., 2019), and HELIOS (Bechtold & Höfle, 2016).

Comprehensive testing of more wood–leaf separation methods based on benchmark datasets and simulated TLS data is the further requirements, which requires the joint efforts of the entire community.

5 | CONCLUSIONS

In this study, we proposed a wood–leaf separation method for TLS point clouds based on the segment-wise classification strategy and compared it with two state-of-the-art methods, that is, the CANUPO and LeWoS. We tested our method using the field-collected TLS datasets in three types of forest plots with different species, as well as an open-access TLS dataset provided by the author of the LeWoS. We compared the methods in terms of accuracy and time efficiency. The results showed that the method proposed in this study achieved the best classification accuracy on average at the forest plot level and improved the time efficiency more than 10 times compared with the point-wise classification methods. This study demonstrates that the segment-wise classification method can greatly improve the efficiency of wood–leaf separation and thus facilitate the application of TLS in the field of forest ecology.

ACKNOWLEDGEMENTS

This work was supported by the National Natural Science Foundation of China (grant nos. 41971380, 42001374). This work was also supported by the Guangxi Natural Science Fund for Innovation Research Team (2019GXNSFGA245001). We also thank the anonymous reviewers for their constructive comments.

CONFLICT OF INTEREST

The authors have no conflicts of interest to declare.

AUTHORS' CONTRIBUTIONS

P.W. conceived the idea, designed the experiments, processed the data and analysed the results; P.W., J.S., S.J., T.W. and W.Z. coordinated the manuscript preparation; all authors contributed to the manuscript writing and editing.

PEER REVIEW

The peer review history for this article is available at https://publons.com/publon/10.1111/2041-210X.13715.

DATA AVAILABILITY STATEMENT

Please contact the authors for the source code and executable program of the proposed method in this study. The open-access manually labelled point clouds are available at https://doi.org/10.5061/dryad.np5hqbzp6 (Wang et al., 2021). The field-collected and manually classified TLS datasets are additionally available at https://doi.org/10.5061/dryad.rfj6q5799 (Wan et al., 2021).

ORCID

Peng Wan https://orcid.org/0000-0002-5366-835X

REFERENCES

Bechtold, S., & Höfle, B. (2016). HELIOS: A multi-purpose LiDAR simulation framework for research, planning and training of laser scanning operations with airborne, ground-based mobile and stationary platforms. *ISPRS Annals of the Photogrammetry, Remote Sensing and Spatial Information Sciences*, *III-3*, 161–168. https://doi.org/10.5194/isprs-annals-III-3-161-2016

Brodu, N., & Lague, D. (2012). 3D terrestrial LiDAR data classification of complex natural scenes using a multi-scale dimensionality criterion: Applications in geomorphology. *ISPRS Journal of Photogrammetry and Remote Sensing*, *68*, 121–134. https://doi.org/10.1016/j.isprsjprs.2012.01.006

Calders, K., Adams, J., Armston, J., Bartholomeus, H., Bauwens, S., Bentley, L. P., Chave, J., Danson, F. M., Demol, M., Disney, M.,

Gaulton, R., Krishna Moorthy, S. M., Levick, S. R., Saarinen, N., Schaaf, C., Stovall, A., Terryn, L., Wilkes, P., & Verbeeck, H. (2020). Terrestrial laser scanning in forest ecology: Expanding the horizon. *Remote Sensing of Environment*, *251*, 112102. https://doi.org/10.1016/j.rse.2020.112102

Chen, Y., Zhang, W., Hu, R., Qi, J., Shao, J., Li, D., Wan, P., Qiao, C., Shen, A., & Yan, G. (2018). Estimation of forest leaf area index using terrestrial laser scanning data and path length distribution model in open-canopy forests. *Agricultural and Forest Meteorology*, *263*, 323–333. https://doi.org/10.1016/j.agrformet.2018.09.006

Côté, J.-F., Widlowski, J.-L., Fournier, R. A., & Verstraete, M. M. (2009). The structural and radiative consistency of three-dimensional tree reconstructions from terrestrial LiDAR. *Remote Sensing of Environment*, *113*(5), 1067–1081. https://doi.org/10.1016/j.rse.2009.01.017

Danson, F. M., Gaulton, R., Armitage, R. P., Disney, M., Gunawan, O., Lewis, P., Pearson, G., & Ramirez, A. F. (2014). Developing a dual-wavelength full-waveform terrestrial laser scanner to characterize forest canopy structure. *Agricultural and Forest Meteorology*, *198*, 7–14. https://doi.org/10.1016/j.agrformet.2014.07.007

Dassot, M., Colin, A., Santenoise, P., Fournier, M., & Constant, T. (2012). Terrestrial laser scanning for measuring the solid wood volume, including branches, of adult standing trees in the forest environment. *Computers and Electronics in Agriculture*, *89*, 86–93. https://doi.org/10.1016/j.compag.2012.08.005

Demantke, J., Mallet, C., David, N., & Vallet, B. (2011). Dimensionality based scale selection in 3D LiDAR point clouds. *International Archives of the Photogrammetry, Remote Sensing and Spatial Information Sciences*, *38*(5), W12.

Disney, M. I., Boni Vicari, M., Burt, A., Calders, K., Lewis, S. L., Raumonen, P., & Wilkes, P. (2018). Weighing trees with lasers: Advances, challenges and opportunities. *Interface Focus*, *8*(2), 20170048. https://doi.org/10.1098/rsfs.2017.0048

Ferrara, R., Virdis, S. G. P., Ventura, A., Ghisu, T., Duce, P., & Pellizzaro, G. (2018). An automated approach for wood-leaf separation from terrestrial LiDAR point clouds using the density based clustering algorithm DBSCAN. *Agricultural and Forest Meteorology*, *262*, 434–444. https://doi.org/10.1016/j.agrformet.2018.04.008

Gastellu-Etchegorry, J.-P., Yin, T., Lauret, N., Grau, E., Rubio, J., Cook, B. D., Morton, D. C., & Sun, G. (2016). Simulation of satellite, airborne and terrestrial LiDAR with DART (I): Waveform simulation with quasi-Monte Carlo ray tracing. *Remote Sensing of Environment*, *184*, 418–435. https://doi.org/10.1016/j.rse.2016.07.010

Girardeau-Montaut, D. (2018). *CloudCompare – 3D point cloud and mesh processing software* (Version 2.10.beta).

Kukko, A., Kaasalainen, S., & Litkey, P. (2008). Effect of incidence angle on laser scanner intensity and surface data. *Applied Optics*, *47*(7), 986–992. https://doi.org/10.1364/AO.47.000986

Lalonde, J., Vandapel, N., Huber, D. F., & Hebert, M. (2006). Natural terrain classification using three-dimensional ladar data for ground robot mobility. *Journal of Field Robotics*, *23*(10), 839–861. https://doi.org/10.1002/rob.20134

Lau, A., Bentley, L. P., Martius, C., Shenkin, A., Bartholomeus, H., Raumonen, P., Malhi, Y., Jackson, T., & Herold, M. (2018). Quantifying branch architecture of tropical trees using terrestrial LiDAR and 3D modelling. *Trees*, *32*(5), 1219–1231. https://doi.org/10.1007/s00468-018-1704-1

Li, Z., Douglas, E., Strahler, A., Schaaf, C., Yang, X., Wang, Z., & Paynter, I. (2013). Separating leaves from trunks and branches with dual-wavelength terrestrial LiDAR scanning. *2013 IEEE International Geoscience and Remote Sensing Symposium-IGARSS*, *2013*(12), B51C–0289). https://ui.adsabs.harvard.edu/abs/2013AGUFM.B51C0289L

Liang, X., Hyyppä, J., Kankare, V., & Holopainen, M. (2013). Stem curve measurement using terrestrial laser scanning. *IEEE Transactions on Geoscience & Remote Sensing*, *52*(3), 1739–1748.

Liang, X., Litkey, P., Hyyppa, J., Kaartinen, H., Vastaranta, M., & Holopainen, M. (2012). Automatic stem mapping using single-scan terrestrial laser scanning. *IEEE Transactions on Geoscience and Remote Sensing*, *50*(2), 661–670. https://doi.org/10.1109/TGRS.2011.2161613

Livny, Y., Yan, F., Olson, M., Chen, B., Zhang, H., & El-Sana, J. (2010). Automatic reconstruction of tree skeletal structures from point clouds. *ACM Transactions on Graphics (TOG)*, *29*(6), 151. https://doi.org/10.1145/1882261.1866177

Ma, L., Zheng, G., Eitel, J. U. H., Moskal, L. M., He, W., & Huang, H. (2016). Improved salient feature-based approach for automatically separating photosynthetic and nonphotosynthetic components within terrestrial LiDAR point cloud data of forest canopies. *IEEE Transactions on Geoscience and Remote Sensing*, *54*(2), 679–696. https://doi.org/10.1109/TGRS.2015.2459716

Pauly, M., Gross, M., & Kobbelt, L. P. (2002). Efficient simplification of point-sampled surfaces. *Proceedings of the conference on Visualization'02*, *2002*(10), 163–170. https://doi.org/10.5555/602099.602123

Pesci, A., & Teza, G. (2008). Effects of surface irregularities on intensity data from laser scanning: An experimental approach. *Annals of Geophysics*, *51*(5–6), 839–848. https://doi.org/10.4401/ag-4462

Pyörälä, J., Liang, X., Saarinen, N., Kankare, V., Wang, Y., Holopainen, M., Hyyppä, J., & Vastaranta, M. (2018). Assessing branching structure for biomass and wood quality estimation using terrestrial laser scanning point clouds. *Canadian Journal of Remote Sensing*, *44*(5), 462–475. https://doi.org/10.1080/07038992.2018.1557040

Qi, J., Xie, D., Yin, T., Yan, G., Gastellu-Etchegorry, J.-P., Li, L., Zhang, W., Mu, X., & Norford, L. K. (2019). LESS: LargE-Scale remote sensing data and image simulation framework over heterogeneous 3D scenes. *Remote Sensing of Environment*, *221*, 695–706. https://doi.org/10.1016/j.rse.2018.11.036

Quammen, D. (2012). Scaling a forest giant. *National Geographic Magazine*, *222*(6), 28–41.

Raumonen, P., Kaasalainen, M., Åkerblom, M., Kaasalainen, S., Kaartinen, H., Vastaranta, M., Holopainen, M., Disney, M., & Lewis, P. (2013). Fast automatic precision tree models from terrestrial laser scanner data. *Remote Sensing*, *5*(2), 491–520. https://doi.org/10.3390/rs5020491

Tao, S., Guo, Q., Xu, S., Su, Y., Li, Y., & Wu, F. (2015). A geometric method for wood-leaf separation using terrestrial and simulated LiDAR data. *Photogrammetric Engineering & Remote Sensing*, *81*(10), 767–776. https://doi.org/10.14358/PERS.81.10.767

Vicari, M. B., Disney, M., Wilkes, P., Burt, A., Calders, K., & Woodgate, W. (2019). Leaf and wood classification framework for terrestrial LiDAR point clouds. *Methods in Ecology and Evolution*, *10*(5), 680–694. https://doi.org/10.1111/2041-210x.13144

Wan, P., Zhang, W., & Jin, S. (2021). Plot-level wood-leaf separation for terrestrial laser scanning point clouds. *Dryad*. https://doi.org/10.5061/dryad.rfj6q5799

Wang, D., Hollaus, M., & Pfeifer, N. (2017). Feasibility of machine learning methods for separating wood and leaf points from terrestrial laser scanning data. *ISPRS Annals of Photogrammetry, Remote Sensing & Spatial Information Sciences*, *4*, 157–164.

Wang, D. I., Momo Takoudjou, S., & Casella, E. (2020). LeWoS: A universal leaf-wood classification method to facilitate the 3D modelling of large tropical trees using terrestrial LiDAR. *Methods in Ecology and Evolution*, *11*(3), 376–389. https://doi.org/10.1111/2041-210X.13342

Wang, D., Takoudjou, S. M., & Casella, E. (2021). LeWoS: A universal leaf-wood classification method to facilitate the 3D modelling of large tropical trees using terrestrial LiDAR. *Dryad*. https://doi.org/10.5061/dryad.np5hqbzp6

Wilkes, P., Lau, A., Disney, M., Calders, K., Burt, A., Gonzalez de Tanago, J., Bartholomeus, H., Brede, B., & Herold, M. (2017). Data acquisition considerations for terrestrial laser scanning of forest plots. *Remote*

Sensing of Environment, *196*, 140–153. https://doi.org/10.1016/j.rse.2017.04.030

Wu, J., Cawse-Nicholson, K., & Aardt, J. van (2013). 3D Tree reconstruction from simulated small footprint waveform lidar. *Photogrammetric Engineering & Remote Sensing*, *79*(12), 1147–1157.

Xi, Z., Hopkinson, C., & Chasmer, L. (2018). Filtering stems and branches from terrestrial laser scanning point clouds using deep 3-D fully convolutional networks. *Remote Sensing*, *10*(8), 1215. https://doi.org/10.3390/rs10081215

Xi, Z., Hopkinson, C., Rood, S. B., & Peddle, D. R. (2020). See the forest and the trees: Effective machine and deep learning algorithms for wood filtering and tree species classification from terrestrial laser scanning. *ISPRS Journal of Photogrammetry and Remote Sensing*, *168*(January), 1–16. https://doi.org/10.1016/j.isprsjprs.2020.08.001

Xu, H., Gossett, N., & Chen, B. (2007). Knowledge and heuristic-based modeling of laser-scanned trees. *ACM Transactions on Graphics (TOG)*, *26*(4), 19. https://doi.org/10.1145/1289603.1289610

Yang, X., Strahler, A. H., Schaaf, C. B., Jupp, D. L. B., Yao, T., Zhao, F., Wang, Z., Culvenor, D. S., Newnham, G. J., Lovell, J. L., Dubayah, R. O., Woodcock, C. E., & Ni-Meister, W. (2013). Three-dimensional forest reconstruction and structural parameter retrievals using a terrestrial full-waveform LiDAR instrument (Echidna®). *Remote Sensing of Environment*, *135*, 36–51. https://doi.org/10.1016/j.rse.2013.03.020

Yao, T., Yang, X., Zhao, F., Wang, Z., Zhang, Q., Jupp, D., Lovell, J., Culvenor, D., Newnham, G., Ni-Meister, W., Schaaf, C., Woodcock, C., Wang, J., Li, X., & Strahler, A. (2011). Measuring forest structure and biomass in New England forest stands using Echidna ground-based LiDAR. *Remote Sensing of Environment*, *115*(11), 2965–2974. https://doi.org/10.1016/j.rse.2010.03.019

Zhang, W., Qi, J., Wan, P., Wang, H., Xie, D., Wang, X., & Yan, G. (2016). An easy-to-use airborne LiDAR data filtering method based on cloth simulation. *Remote Sensing*, *8*(6), 501. https://doi.org/10.3390/rs8060501

Zhao, F., Yang, X., Schull, M. A., Román-Colón, M. O., Yao, T., Wang, Z., Zhang, Q., Jupp, D. L. B., Lovell, J. L., Culvenor, D. S., Newnham, G. J., Richardson, A. D., Ni-Meister, W., Schaaf, C. L., Woodcock, C. E., & Strahler, A. H. (2011). Measuring effective leaf area index, foliage profile, and stand height in New England forest stands using a full-waveform ground-based lidar. *Remote Sensing of Environment*, *115*(11), 2954–2964. https://doi.org/10.1016/j.rse.2010.08.030

Zhang, W., Wan, P., Wang, T., Cai, S., Chen, Y., Jin, X., & Yan, G. (2019). A novel approach for the detection of standing tree stems from plot-level terrestrial laser scanning data. *Remote Sensing*, *11*(2), 211. https://doi.org/10.3390/rs11020211

Zhu, X., Skidmore, A. K., Darvishzadeh, R., Niemann, K. O., Liu, J., Shi, Y., & Wang, T. (2018). Foliar and woody materials discriminated using terrestrial LiDAR in a mixed natural forest. *International Journal of Applied Earth Observation and Geoinformation*, *64*, 43–50. https://doi.org/10.1016/j.jag.2017.09.004

How to cite this article: Wan, P., Shao, J., Jin, S., Wang, T., Yang, S., Yan, G., & Zhang, W. (2021). A novel and efficient method for wood–leaf separation from terrestrial laser scanning point clouds at the forest plot level. *Methods in Ecology and Evolution*, 00, 1–14. https://doi.org/10.1111/2041-210X.13715